A Fully Automatic Pipeline to Optimize Radio-Frequency Coil Design Using the Ultimate Intrinsic Signal-to-Noise Ratio as the Benchmark

José E. Cruz Serrallés[1], Ilias I. Giannakopoulos[1], Siqi Wang[2], Damien Chen[2], Xin Zhao[2], Daniel Zint[2], Daniele Panozzo[2], Denis Zorin[2], and Riccardo Lattanzi[1,3]

[1]Center for Biomedical Imaging, Department of Radiology, New York University Grossman School of Medicine, New York, NY, United States, [2]Courant Institute of Mathematical Sciences, New York University, New York, NY, United States, [3]Center for Advanced Imaging Innovation and Research (CAI2R), New York University Grossman School of Medicine, New York, NY, United States

Synopsis

Motivation: Despite the crucial importance of radio-frequency coils, the practical coil design process has remained a largely empirical one.

Goal(s): To introduce a fully automatic procedure to optimize coil design using the ultimate intrinsic signal-to-noise ratio (UISNR) as the reference.

Approach: We developed an intuitive user interface to parameterize and mesh coils, and implemented automatic tune-match-decoupling. We used MARIE to calculate coil SNR and the UISNR inside a head model. We optimized the size and position of loop coils with the goal of maximizing SNR/UISNR at target locations.

Results: The optimization converged to coil configurations resembling the ideal current patterns.

Impact: Optimizing the design of receive coil arrays can improve image quality and parallel imaging performance. This work demonstrates the first fully automatic approach to design receive coils that can approach the ultimate intrinsic signal-to-noise ratio.

Introduction

The radiative characteristics of a radio-frequency (RF) receive coil dictate the signal-to-noise ratio (SNR) in the received signal and hence in magnetic resonance (MR) images. Additionally, arrays of multiple receive coils enable parallel imaging, a process whereby scan time is reduced by exploiting the spatial locality of individual coils to reconstruct MR images from undersampled k-space acquisitions[1,2]. RF coils are usually designed by hand and are occasionally simulated using commercial tools before building a prototype. This manual design process leaves room for potential performance gains that could be achieved by optimizing programmatically over geometric parameters.

While the main obstacle to optimization is the large parameter space, other challenges have limited the exploration of this approach. The lack of an absolute benchmark means that coil performance is assessed relative only to existing geometries. Simulation times of days to weeks for dense arrays[3] render programmatic design prohibitively time-consuming. Another limitation is the need to remesh the geometry and to tune, match, and decouple the coils reliably while optimizing.

Despite these hurdles, techniques to facilitate programmatic coil design have been developed, not only for receive coils but also for transmit and gradient coils[4,5]. In this work, we propose a novel approach for designing receive coil arrays programmatically, with open-source simulation and meshing tools, tuning & decoupling algorithms, and the ultimate intrinsic signal-to-noise ratio (UISNR)[6] as a benchmark for performance.

Methods

We calculated the electromagnetic fields produced by RF coils inside a numerical body model using MARIE[7] with our own modifications, such as compressed VIE operators[8,9] and improved SIE assembly[10]. We adapted the Magnetic Resonance Green's Function (MRGF)[11] approach to highly accelerate coil simulations. We parameterized loop coils using control points, interpolating using b-splines. We developed a graphical user interface (GUI) to design and mesh coils on a two-dimensional (u, v) plane (Fig.1). The GUI enabled us to automatically map coils onto a 3D substrate surface surrounding the head using the Scalable Locally Injective Maps algorithm[12]. We attached ideal current sources at each port and parallel capacitors at the non-port terminals to tune and decouple the coils by minimizing the reactance at each port to force each loop to resonate. We first optimized capacitors using the Particle Swarm algorithm and then Newton's method to refine the

solution. We calculated the UISNR with MARIE using a numerical basis over a closed surface encompassing the coil substrate[13,14]. We maximized the ratio of the L_2 norms of SNR and UISNR in a region-of-interest (RoI). We estimated parameter derivatives using finite-differences and alternated coordinate descent and gradient descent when optimizing the geometry.

To test our coil design optimization approach, we performed numerical experiments in which we sought to maximize the SNR in a single-voxel RoI in the posterior region of the brain or in a two-voxel RoI with an additional voxel in the anterior region. We increased the number of loops and qualitatively compared our solutions with the ideal current patterns (ICP)[14,15] associated with the UISNR (Fig.2).

Results and Discussion

In the first experiment, we optimized over the radius and position of one loop. The evolution of the geometry and the SNR to UISNR ratios are shown in Fig.3. The loop minimized its distance from the RoI, achieving 46.7% of the UISNR. In the second experiment, we optimized over parameters of three loops for the same RoI (Fig.4). The three loops migrated toward the back of the head, achieving 83.2% absolute performance at the RoI and with the current distribution closely resembling the combined loop and figure eight configuration seen in the ICP (Fig.2). In the third experiment, we added an anterior voxel to the RoI and optimized over the parameters of four loops. Interestingly, three loops closely resembled the optimal three-loop configuration, while the fourth loop migrated toward the front (Fig.5), achieving 84.2% and 59.1% absolute performance in the back and front, respectively.

Conclusion

Maximizing the SNR of receive coil arrays improves MR image quality and enables larger acceleration factors. We presented the first fully automatic pipeline to optimize coil design using UISNR as the performance benchmark. We overcame the challenges associated with programmatic coil design by extending the capabilities of MARIE, implementing a tailored meshing strategy, and automatizing tuning and decoupling using optimization. We demonstrated the effectiveness of our approach with numerical experiments using an increasing number of loops. Each trial resulted in a higher SNR than the previous trial, approaching the limit set by UISNR. Future work includes optimizing dense receive arrays, optimizing transmit arrays, and using adjoint methods to accelerate the optimization and enable searching over a wider parameter space.

Acknowledgements

The first two authors contributed equally to this work. This work was supported by NIH R01 EB024536, NSF 2313156, NIH K99 EB035163, and performed under the Rubric of the Center for Advanced Imaging Innovation and Research (CAI2R, www.cai2r.net), an NIBIB National Center for Biomedical Imaging and Bioengineering (NIH P41 EB017183).

References

1. Sodickson, D. K., & Manning, W. J. (1997). Simultaneous acquisition of spatial harmonics (SMASH): fast imaging with radiofrequency coil arrays. Magnetic resonance in medicine, 38(4), 591-603.
2. Pruessmann, K. P., Weiger, M., Scheidegger, M. B., & Boesiger, P. (1999). SENSE: sensitivity encoding for fast MRI. Magnetic Resonance in Medicine: An Official Journal of the International Society for Magnetic Resonance in Medicine, 42(5), 952-962.
3. Zhang, B., Radder, J., Giannakopoulos, I., Grant, A., Lagore, R., Waks, M., Tavaf, N., Van de Moortele, P.-F., Adriany, G., Sadeghi-Tarakameh, A., Eryaman, Y., Lattanzi, R., & Uğurbil, K. (2024). Performance of receive head arrays versus ultimate intrinsic SNR at 7 T and 10.5 T. Magnetic resonance in medicine.
4. Serrallés, J. E. C., Adalsteinsson, E., Wald, L. L., & Daniel, L. (2020). Rapid parametric optimization of transmit coil arrays: a proof-of-concept. In The International Society for Magnetic Resonance in Medicine (p. 4262).
5. Serrallés, J. E. C., Adalsteinsson, E., Wald, L. L., & Daniel, L. (2021). Parametric coil optimization via global optimization. In Proc. ISMRM (p. 1399).
6. Lattanzi, R., Grant, A. K., Polimeni, J. R., Ohliger, M. A., Wiggins, G. C., Wald, L. L., & Sodickson, D. K. (2010). Performance evaluation of a 32-element head array with respect to the ultimate intrinsic SNR. NMR in Biomedicine: An International Journal Devoted to the Development and Application of Magnetic Resonance In vivo, 23(2), 142-151.
7. Guryev, G. D., Milshteyn, E., Giannakopoulos, I. I., Lattanzi, R., Wald, L. L., Adalsteinsson, E., & White, J. K.

(2022). MARIE 2.0: a perturbation matrix based patient-specific MRI field simulator. IEEE Transactions on Biomedical Engineering, 70(5), 1575-1586.
8. Giannakopoulos, I. I., Guryev, G. D., Serrallés, J. E. C., Georgakis, I. P., Daniel, L., White, J. K., & Lattanzi, R. (2021). Compression of volume-surface integral equation matrices via Tucker decomposition for magnetic resonance applications. IEEE transactions on antennas and propagation, 70(1), 459-471.
9. Giannakopoulos, I. I., Guryev, G. D., Serrallés, J. E. C., Paška, J., Zhang, B., Daniel, L., White, J. K., Collins, C. M., & Lattanzi, R. (2022). A hybrid volume-surface integral equation method for rapid electromagnetic simulations in MRI. IEEE Transactions on Biomedical Engineering, 70(1), 105-114.
10. Serrallés, J. E. C., Giannakopoulos, I. I., & Lattanzi, R. (2024). On the Extension of MARIE Coil Simulation to Low Frequencies and Arbitrarily Fine Meshes. In Proceedings of the 32nd Annual Meeting of ISMRM, Singapore (p. 2843).
11. Villena, J. F., Polimeridis, A. G., Eryaman, Y., Adalsteinsson, E., Wald, L. L., White, J. K., & Daniel, L. (2016). Fast electromagnetic analysis of MRI transmit RF coils based on accelerated integral equation methods. IEEE Transactions on Biomedical Engineering, 63(11), 2250-2261.
12. Rabinovich, M., Poranne, R., Panozzo, D., & Sorkine-Hornung, O. (2017). Scalable locally injective mappings. ACM Transactions on Graphics (TOG), 36(4), 1.
13. Georgakis, I. P., Villena, J. F., Polimeridis, A. G., & Lattanzi, R. (2022). Novel numerical basis sets for electromagnetic field expansion in arbitrary inhomogeneous objects. IEEE transactions on antennas and propagation, 70(9), 8227-8241.
14. Giannakopoulos, I. I., Georgakis, I. P., Sodickson, D. K., & Lattanzi, R. (2024). Computational methods for the estimation of ideal current patterns in realistic human models. Magnetic resonance in medicine 91.2 (2024): 760-772.
15. Lattanzi, R., & Sodickson, D. K. (2012). Ideal current patterns yielding optimal signal-to-noise ratio and specific absorption rate in magnetic resonance imaging: computational methods and physical insights. Magnetic resonance in medicine, 68(1), 286-304.

Figures

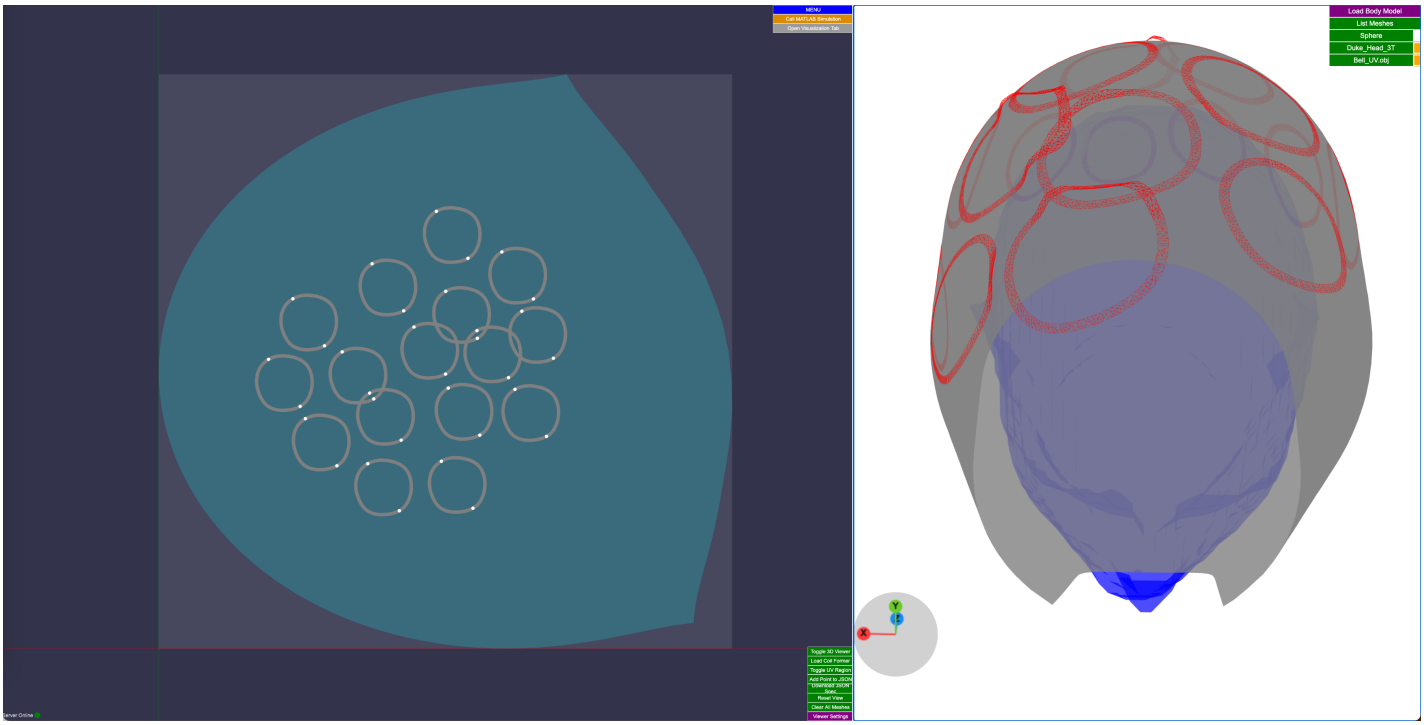

Figure 1. Graphical user interface for coil design and visualization. Coil geometries can be defined in the 2D (u, v) domain (left) and conveniently project onto the desired coil support surface (right) via the SLIM algorithm.

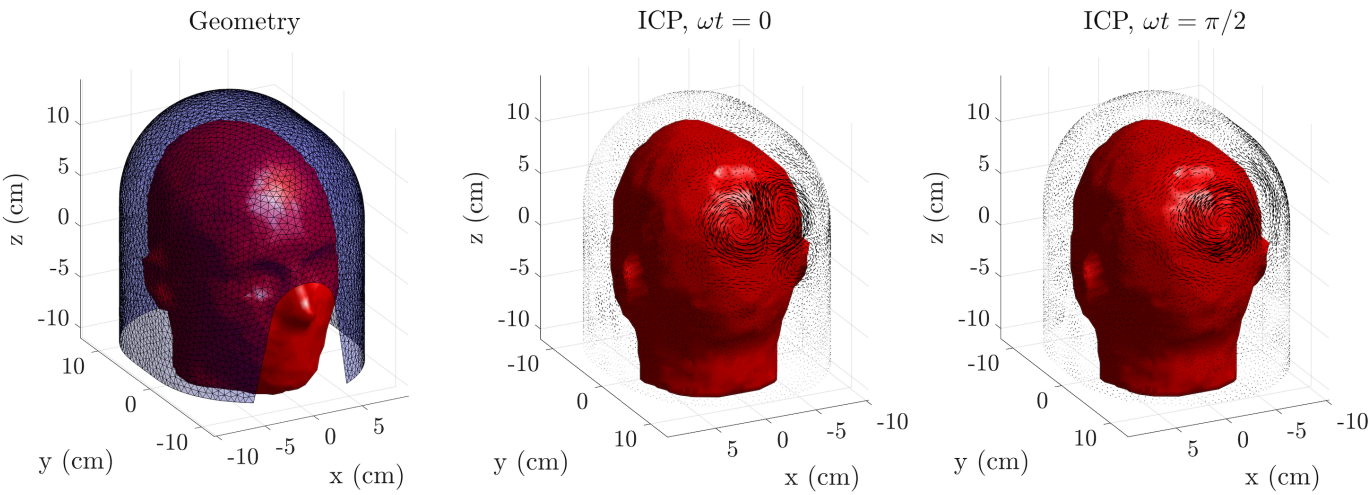

Figure 2. Realistic coil former surrounding the head model (left). All studied coils were mapped onto the same coil former. The former also served as a current-bearing surface for the estimation of the ideal current patterns. Temporal snapshots of the ideal current patterns yielding optimal signal-to-noise ratio at the voxel in the back of the head for two time-points are shown in the middle ($\omega t = 0$) and right ($\omega t = \frac{\pi}{2}$).

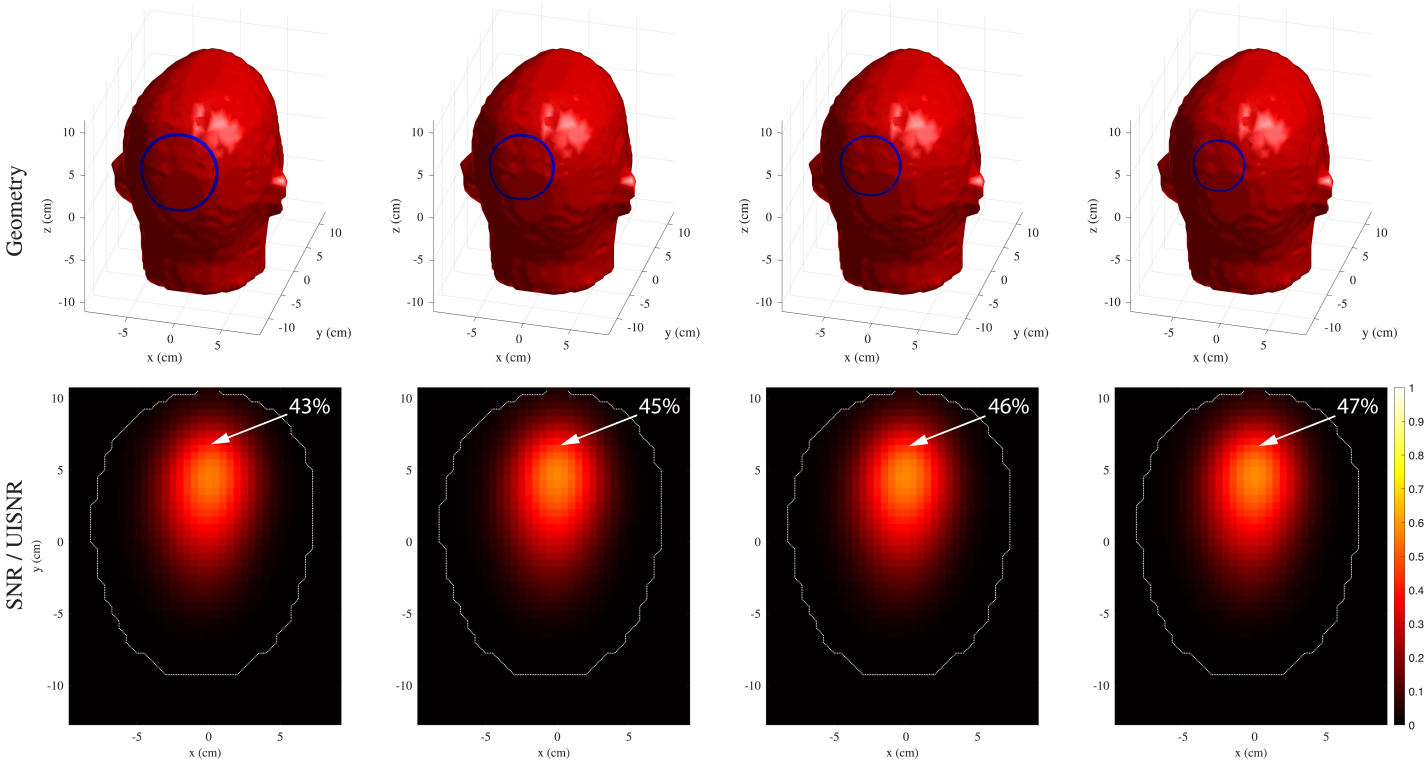

Figure 3. Evolution of single loop coil geometry during the optimization (top) and associated SNR to UISNR ratio map over an axial slice containing the target voxel in the back of the head (bottom). Left-to-right: Iterations 1, 25, 50, and 100 (final) of grid search over radius, u coordinate, and v coordinate. The SNR to UISNR ratio at the voxel of interest increased steadily from 43% to 47% over 100 iterations.

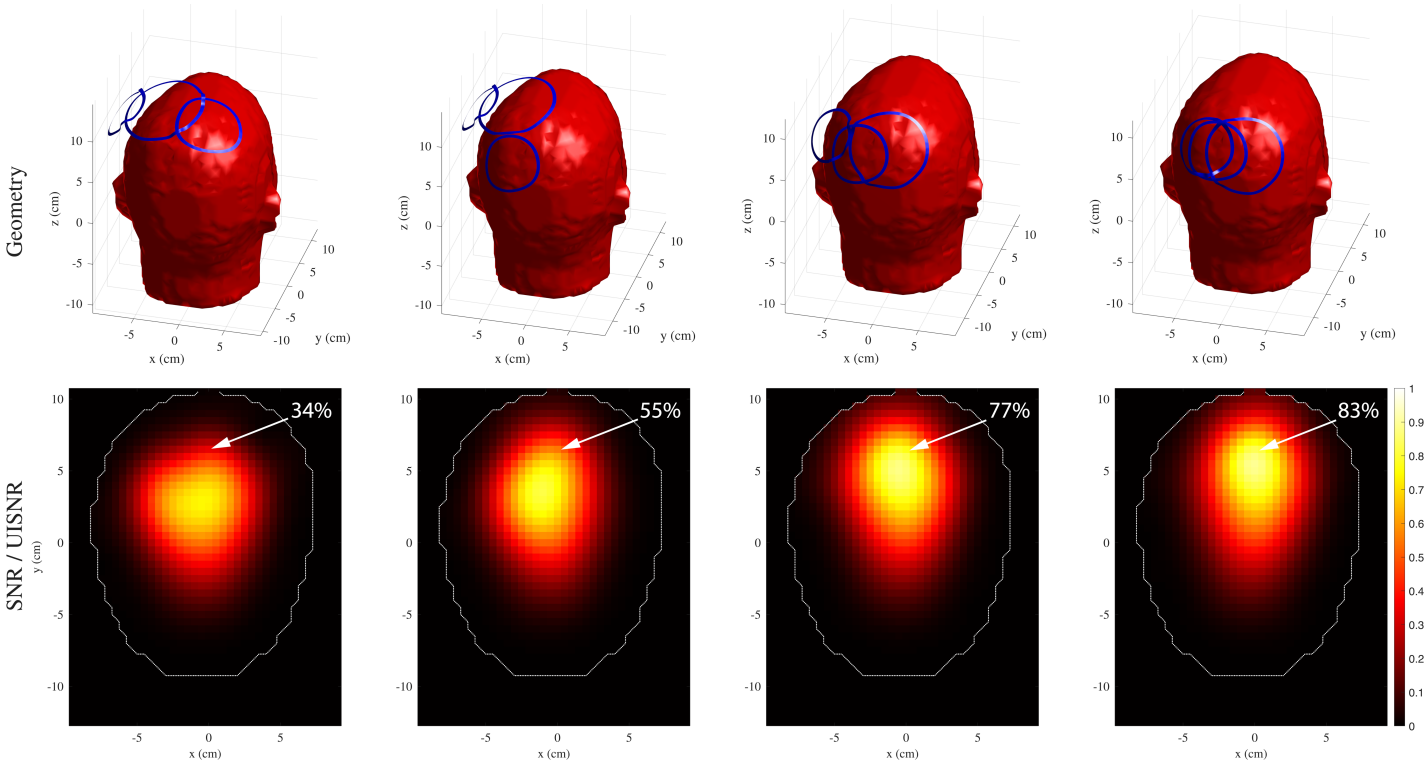

Figure 4. Evolution of three-loop coil array geometry (top) and associated SNR to UISNR ratio maps over an axial slice containing the target voxel (bottom). Left-to-right: Iterations 1, 3, and 7 of initial coordinate descent, and Iteration 53 (final) of gradient descent. The absolute performance at the target voxel increased steadily from 34% to 77% during coordinate descent and gained an additional 6% during gradient descent, settling on 83% after the final iteration.

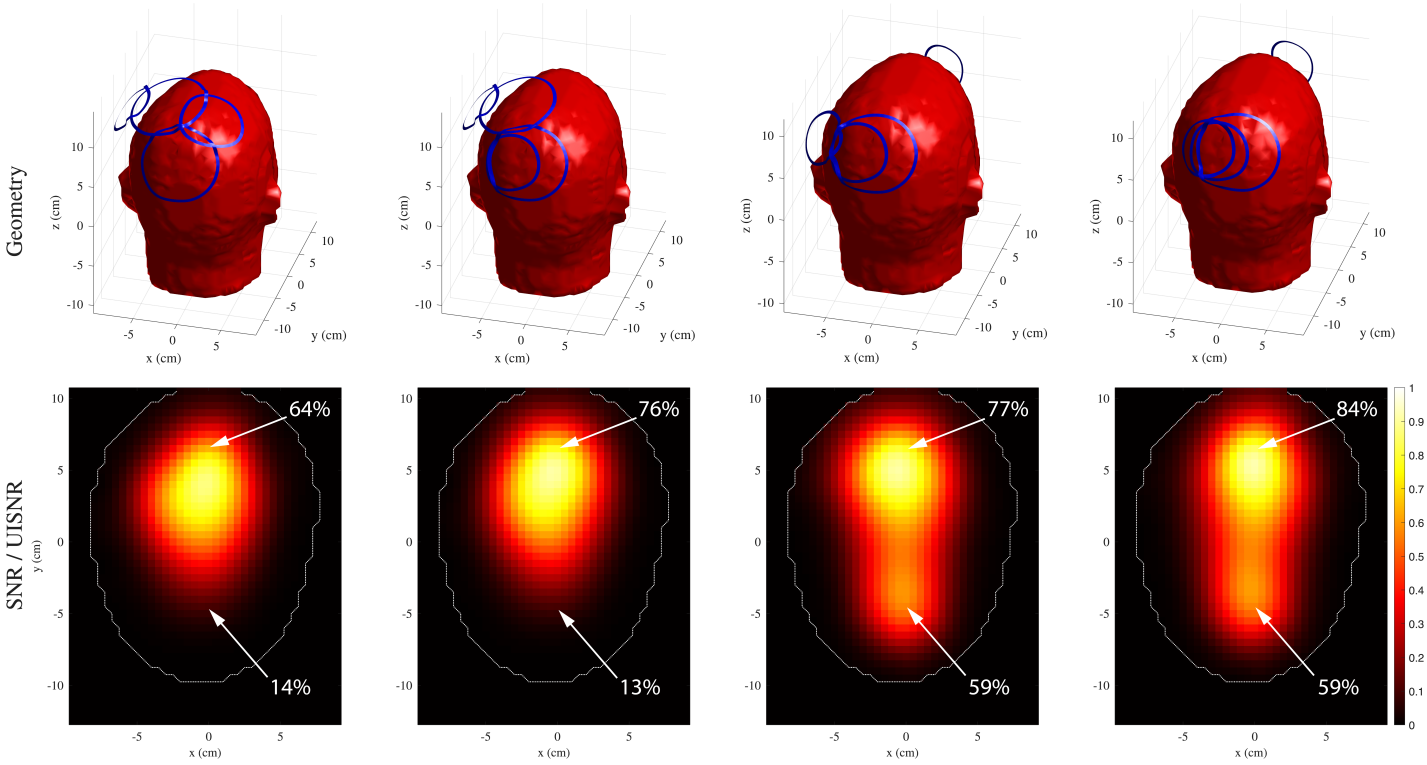

Figure 5. Evolution of four-loop coil array geometry (top) and associated SNR to UISNR ratio maps over an axial slice containing two target voxels, at the front and back of the head (bottom). Left-to-right: Iterations 1, 3, and 6 of initial coordinate descent, and Iteration 68 (final) of gradient descent. The absolute performance at the anterior voxel increased steadily from 64% to 77% during coordinate descent and gained an additional 7% during gradient descent, settling on 84% after the final iteration.